2008

Spatial distribution of forest aboveground biomass estimated from remote sensing and forest inventory data in New England, USA.

Daolan Zheng
University of New Hampshire

Linda S. Heath
USDA Forest Service

Mark J. Ducey
University of New Hampshire, mark.ducey@unh.edu

Recommended Citation

Zheng, D., Heath, L.S., Ducey, M.J. Spatial distribution of forest aboveground biomass estimated from remote sensing and forest inventory data in New England, USA. (2008) Journal of Applied Remote Sensing, 2 (1), art. no. 021502, . doi: 10.1117/1.2940686

Spatial distribution of forest aboveground biomass estimated from remote sensing and forest inventory data in New England, USA

Daolan Zheng[a], Linda S. Heath[b], and Mark J. Ducey[a]

[a] Department of Natural Resources, University of New Hampshire, Durham, NH 03824, USA
daolan.zheng@unh.edu, mjducey@unh.edu
[b] USDA Forest Service, Northern Research Station, Durham, NH 03824, USA
lheath@fs.fed.us

Abstract. We combined satellite (Landsat 7 and Moderate Resolution Imaging Spectrometer) and U.S. Department of Agriculture forest inventory and analysis (FIA) data to estimate forest aboveground biomass (AGB) across New England, USA. This is practical for large-scale carbon studies and may reduce uncertainty of AGB estimates. We estimate that total regional forest AGB was 1,867 teragram (10^{12}, dry weight) in 2001, with a mean AGB density of 120 Mg/ha (Standard deviation = 54 Mg/ha) ranging from 15 to 240 Mg/ha within a 95% percentile. The majority of regional AGB density was in the range of 80 to 160 Mg/ha (58.2%). High AGB densities were observed along the Appalachian Mountains from northwestern Connecticut to the Green Mountains in Vermont and White Mountains in New Hampshire, while low AGB densities were concentrated in the Downeast area of Maine (ME) and the Cape Cod area of Massachusetts (MA). At the state level, the averaged difference in mean AGB densities between simulated and FIA (as reference) was -2.0% ranging from 0% to -4.2% with a standard error of 3.2%. Within the 95% confidence interval the differences between FIA and simulated AGB densities ranged from 0 to 6% (absolute value). Our study may provide useful information for regional fuel-loading estimates.

Key Words: Reflectance, stand age, ratio map, vegetation indices, biomass density.

1 INTRODUCTION

Forests play the largest role among different terrestrial ecosystems in the global carbon cycle by sequestering a large quantity of carbon, which mitigates the increase of atmospheric carbon concentration. Globally, estimates of forest carbon stocks range from 77 to 82% of the total terrestrial carbon stock [1] Quantifying carbon in forests is increasingly important for monitoring and reporting requirements, be they at a national or continental level and legally-binding [2-3] or voluntary [4], or of interest to States [5] The various needs include the ability to assign forest carbon to a location that allows for analysis of previous land use (to determine whether the carbon was due to afforestation or deforestation for instance), and a consistent scaling procedure so that large area estimates within a region can be summed and are consistent with the area of the region.

On the one hand, remote sensing approaches that allow for multitemporal monitoring across a continuous landscape provide promising and reliable data sources for studying and quantifying ecosystem properties and processes over large scales [6-10] On the other hand, a statistically designed natural resources survey with a large component of field measurements, such as the U.S. Department of Agriculture (USDA) Forest Service, Forest Inventory and Analyses (FIA) can be used to provide forest carbon estimates that are accurate and verifiable [11] These plot data, located in a systematic way across the region (approximately every 5 km in forestland, on average), provide unbiased estimates of areal means and totals. The general principles of design-unbiased inference from this type of systematic survey are given

 [DOI: 10.1117/1.2940686]
Received 8 Oct 2007; accepted 9 May 2008; published 20 May 2008 [CCC: 19313195/2008/$25.00]

by Thompson [12], while model-unbiased estimators specific to FIA data are given by Bechtold and Patterson [13] However, the FIA data are scattered points and thus have limited usage for continued landscapes.

Integrating remote sensing (spatially-explicit observations) and national resources inventory data may provide more consistent, reliable, and comparable spatial analyses across landscapes [14], and provide a framework of improved forest carbon estimates for ecological modeling and fuel-loading prediction [15-16]

In recent decades, a remote sensing component has been used in the FIA program (Phase I) to classify land as forest or non-forest and to measure fragmentation [17] However, more information such as surface reflectance, the normalized difference vegetation index (NDVI), corrected NDVI (NDVIc) can be gleaned from remote sensing to improve terrestrial ecosystem carbon analyses. Many studies have demonstrated that remote sensing data collected from different sensors at various scales (e.g. from 1-m IKONOS to 1-km Moderate Resolution Imaging Spectroradiometer -- MODIS) can be directly or indirectly used for estimating aboveground forest biomass or other landscape characteristics at various scales depending on study purpose and scope [10, 18-23]

Directly coupling coarser resolution remote sensing data with FIA plot data, however, is inappropriate because of the discrepancy in spatial resolutions between the two data sources [24-25] For example, in contrast to MODIS data with the finest resolution of 250 m, or 62,500 m^2, each FIA phase-2 permanent plot covers approximately 672 m^2 [13] Therefore, it is more appropriate to link plot observations with 30-m Landsat 7 Enhanced Thematic Mapper plus (ETM+) data.

This study focuses on aboveground biomass (AGB, dry weight) because it comprises 75 to 85% of the carbon stocks of forests depending on forest type worldwide [26] While the New England area of the USA accounts for about 2.0% of the nation's land area, the area is 84% forested and represents 4.5% of the nation's forestland [27] Thus, this area may possess disproportional importance in the nation's forest ecosystem carbon studies. Our study objectives are to: 1) present and demonstrate a method in which remote sensing imagery and FIA field data can be integrated to estimate regional AGB and stand age in New England, USA; 2) illustrate the spatial patterns of stand age and AGB densities in the region, as well as the AGB distributions by broad forest types; and 3) provide baseline AGB estimates of the region for use in more comprehensive carbon studies.

2 MATERIALS AND METHODS

We model regional AGB using remote sensing data and USDA Forest Service FIA data. We use two sets of remote sensing data, one with a smaller pixel size (ETM+, 30m) that is closer to the size of the FIA plot for model development, and the other with a larger pixel size (MODIS, 1km) for model parameterizations and application at regional scale. Detailed steps (see Fig. 1) include: 1) establishing an AGB model within a limited portion of the region using ETM+ data that has a pixel size more comparable to the FIA field plot footprint; 2) conducting spectral calibrations between ETM+ and MODIS sensors so the ETM+ based model can be applied to entire region using MODIS data; 3) creating a regional age map (required input of the AGB model) derived from remotely sensed information and constrained by the regional stand-age structure obtained from FIA data; and 4) adjusting modeled AGB using FIA-derived county means through a ratio map.

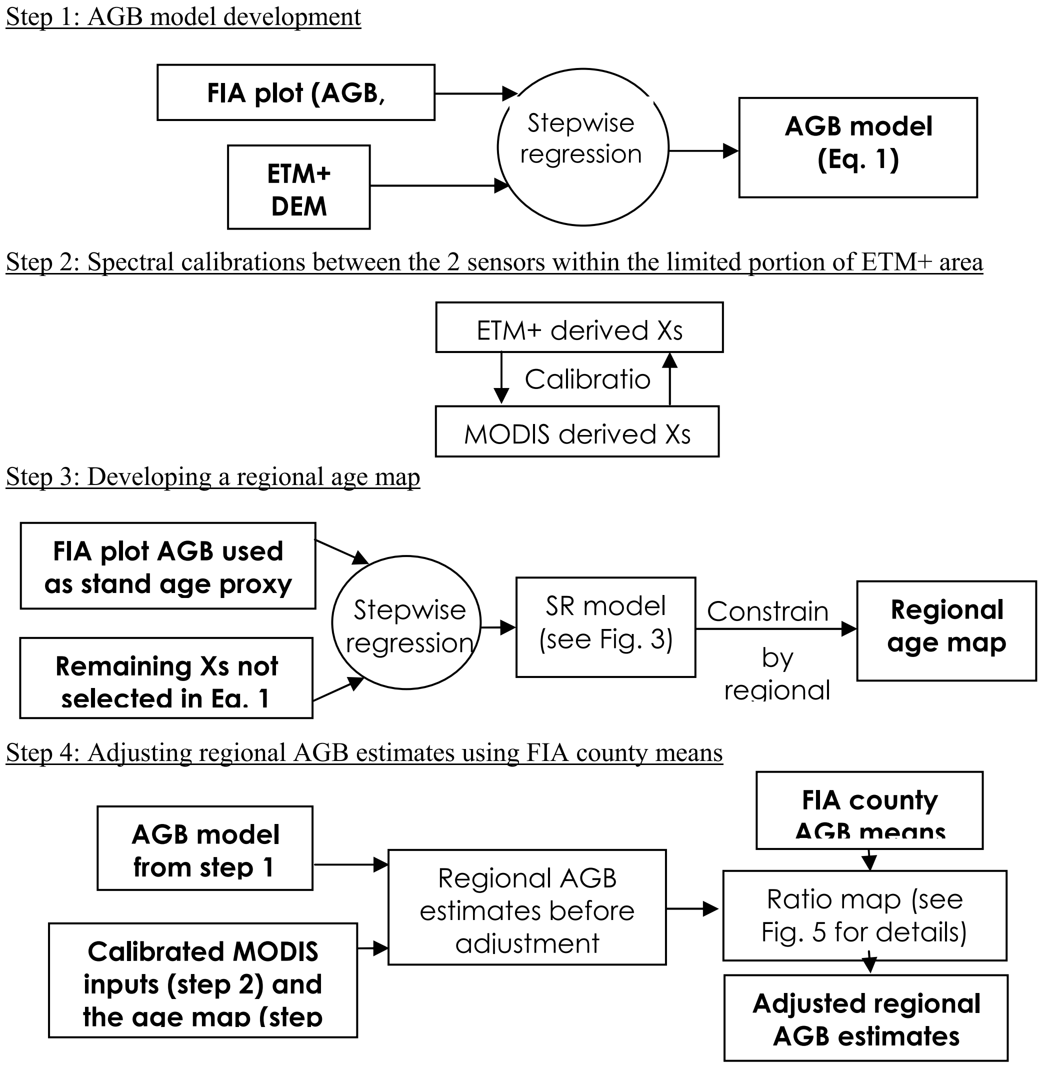

Fig. 1. Flow chart of steps used for estimating regional forest aboveground biomass (AGB). Rectangular boxes with **bolded** text are inputs and final output; the circle and other boxes are function and intermediate products. See text for more information and Fig. 8b for the limited portion of the region within which the model was developed using ETM+ data.

2.1 Study area

Our study area is located in New England, USA, with a total land area of 181,440 km^2 (Fig. 2). About eighty-four percent is forested according to the MODIS land-cover map of 2001 (MODIS12Q1 type 2 classification). The area is characterized by rolling hills, mountains, and a jagged coastline as a result of retreating ice sheets that shaped the landscape thousands of years ago. Elevation ranges from sea level to 1,917 m at Mount Washington in NH. Four dominant forest types collectively cover 86% of the area's forestland: a) spruce-fir in northern ME and at high elevation; b) white/red/jack pine along the coast line from southern ME to RI including central MA; c) oak/hickory in CT and most of RI; and 4) maple/beech/birch in southwestern NH and western VT [27]

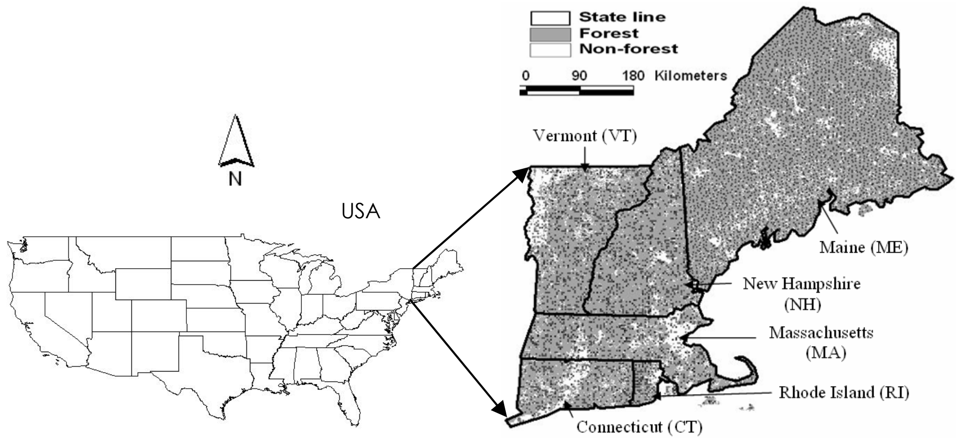

Fig. 2. Six New England States with a general distribution of two broad cover types (forest vs. non-forest) based on the MODIS 2001 land-cover map and the approximate locations (dots in dark) of the FIA plots.

The climate in New England varies throughout the region, but is known for its unpredictability regionwide. Maine, NH, and VT, in the north, have a humid continental short summer climate, with relatively cool summers and long, cold winters. Connecticut, MA, and RI, in the south, have a humid, continental, long summer climate, with hot summers and cold winters. Long-term climatic data (1961-1990) at half-degree resolution suggest that annual mean temperature across the region is 5.7 °C with monthly mean temperatures of -8.9 °C and 19.2 °C in January and July, respectively; annual mean total precipitation is 1,121 mm [28] The average rainfall for most of the region ranges from 1,000 to 1,500 mm a year, with the northern parts of VT and ME notably lower, ranging from 500 to 1,000 mm.

2.2 Ground AGB calculations using FIA data

The AGB in this study is defined as dry weight biomass of all live trees with diameter breast height (dbh) >= 2.5 cm including stem, branch, and foliage. Our AGB calculations did not include FIA plots with TPACURR = 0 (current trees per acre), and we excluded understory biomass because it is estimated to be minor. For example, second growth maple-beech-birch stands have only about 3.5 Mg/ha understory biomass [29], or 2.7% of AGB on average.

Plot AGB was calculated using FIA tree-level data measured in 2001, if available, or interpolated between two surveys before and after 2001 in the 6 New England states. We used the true plot locations as they are recorded in the FIA data. Given at least 180 GPS readings at the plot center, no individual position has an error larger than 21.4 m and the error of all the averaged readings is far less [30] We selected the year of 2001 for consistency with a previous AGB study in the Great Lakes region [10] so comparisons of AGB estimates among regions can be made in future studies. Plot AGB was obtained by estimating AGB values for all individual trees within the plot as a function of dbh using the 10 generalized regression models developed by Jenkins et al. [31] for all North American tree species. All AGB calculations were appropriately converted to biomass density (Mg/ha) [13] Stand age information for a given plot was also recorded if it was available from the FIA dataset.

2.3 Remote sensing data

A full ETM+ image of 2001 covering parts of VT, NH, and MA was acquired for September 5 (still presenting the full canopy). The image was geo-referenced and the raw satellite data in each ETM+ band (except the thermal and panchromatic bands) were converted to reflectance using an exo-atmospheric model before vegetation indices were calculated [32]

MODIS (1-km resolution) reflectance composite data in early September, 2001 (MOD09A1) and land-cover map of 2001 (MOD12Q1) across the region were obtained online [33] We used the MODIS land-cover map (with classification system type 2) to mask out forest (including evergreen, deciduous, and mixed forests) from non-forest (including all the other types) for data analyses (Fig. 2).

2.4 Model development

The calculated plot-level AGB values within the ETM+ scene were directly coupled with reflectance in six bands (blue, green, red, near infrared (NIR), and two middle infrared channels), three remote-sensing derived indices, DEM, and the recorded stand ages for the plots (a total of 11 independent variables) [34] A multi-regression model was developed using stepwise (forward) regression approach, one of the commonly used methods for estimating AGB from remote sensing [35-36] This approach can prevent an independent variable from entering the model if it is strongly related with a variable that has been previously selected [37] The three vegetation indices were: 1) Normalized Difference Vegetation Index (NDVI) calculated from reflectance (ρ) in red and near infrared channels $((\rho_{NIR} - \rho_{red}) / (\rho_{NIR} + \rho_{red})$, [38]; 2) simple ratio (SR, ρ_{NIR} / ρ_{red}); and 3) NDVIc calculated from NDVI * $[1 - (mIR - mIR_{min}) / (mIR_{max} - mIR_{min})]$ [39] where mIR is middle infrared reflectance in the 1,600 nm wavelength. These indices have been successfully used for forest production and biomass studies at various degrees [10, 20, 40-42] DEM (30-m resolution) data were downloaded from the USGS National Elevation Dataset [43]

A total of 499 FIA plots were identified within the ETM+ scene, which had values of AGB and all 11 independent variables. We systematically divided these plots into two groups (even number vs. odd number). One group was used for model development (Fig. 1, step 1) and the other group was reserved for model validation. Effect of broad forest types (deciduous vs. evergreen) on AGB estimates was also examined to determine whether a separate model was needed for each forest type.

2.5 Spectral calibrations between two sensors

The use of finer spatial resolution data is an essential step to integrate ground measurements with coarse spatial resolution data. To perform this step, the relationship of spectral responses was examined [44-45] We conducted internal spectral calibrations between 30-m ETM+ and 1-km MODIS data (Fig. 1, step 2) due to the differences in spatial and spectral resolutions between the two sensors [24, 45] We examined the correlations of blue, red, near infrared, middle infrared reflectance after finer ETM+ data were aggregated to the same resolution (1-km) of MODIS data within the area of ETM+ scene. The resulting spectral relationships for the identified bands within the ETM+ scene were used for calibrating MODIS data across the region. These bands are either being used directly as driving variables in the model or indirectly for calculating various vegetation indices that drive the model (Table 1). Such calibrations are necessary because: 1) the models are established using ETM+ data, and 2) remotely sensed information between the 2 sensors is not identical, even for the same targets.

Table 1. Correlation coefficients for reflectance of individual bands and vegetation indices between MODIS and ETM+.

Band/Indices	Bandwidth (nm) ETM+	MODIS	r	Sample size (N)
Blue	450-520	459-479	0.509	28876
Red	630-690	620-670	0.654	29008
Infrared	780-900	841-876	0.742	29008
Middle Inf.	1550-1750	1628-1652	0.649	29008
NDVI			0.682	28892
NDVIc			0.524	28892

2.6 Creation of a regional age map

Field and the resulting model data suggest that AGB is a function of stand age across the region as well as for hardwood dominated Northern US forests in general [10, 29] However, the age values for all plots used in the model development came from point observations. Therefore, generating a spatially-explicit age map is a necessary step for AGB estimation across the region.

In addition to the plots available for model development and validation, 378 plots within the ETM+ scene that had AGB values but no age information were identified. We used these AGB values as a proxy for stand ages and correlated the AGB values with remotely sensed information. Previous studies have shown that stand age shows a good relationship with the NIR band or the combination of red and NIR [10, 45-47] In this study we found that simple ratio (SR) of reflectance in NIR and red bands was the variable (among the remaining variables that were not selected in the equation 1) most related to the plot AGB observations in the group used as a proxy for age. A large sample size allowed us to construct a more restrictive relationship between AGB (age proxy) and SR (Fig. 3). First, we calculated the ratio between AGB and SR and excluded all pairs whose ratio values were out of the range (mean ± one standard deviation (Std.)). Second, for the remaining pairs, we calculated the AGB means for each of the SR values at the precision of one digit after the decimal point (e.g., from 1.2 to 12.6). Ratioing enables outlying data to be quantified. The purpose of the above procedures was for a robust extrapolation of SR values across the region, not to estimate r^2 value in the initial population.

The predicted AGB values (age proxy) resulting from the SR model (using the calibrated MODIS input) were converted to a stand age map based on the age structure developed from 5,502 FIA plots across the 6 New England states following the method of Schulte et al. [48] (Fig. 1, step 3). The threshold values of AGB estimates used for age-class conversions were determined in such a way that distributions of the converted age classes matched the frequency distributions calculated from the FIA (Fig. 4). The underlying principle for such a conversion is that AGB is positively correlated to stand age before reaching a plateau [10, 49-52] We assumed that locations with higher biomass estimates indicate denser and older forest stands [45, 53-55] Finally, we tested the colinearity between our age variable resulting from SR and the other remotely sensed variables presented in Eq. 1.

2.7 Adjusting satellite-derived AGB using FIA-derived county means

We used the county AGB means derived from the FIA plots to adjust MODIS-based regional AGB estimates with a ratio map (Fig. 5; Fig. 1, step 4). This application takes the advantages of remote sensing data that retain the information of spatially-explicit variation within a given area and the improved accuracy from field inventory data containing large number of samples but collected at scattered points within the area. We used state means to calculate the ratio map so as to keep the integrity of spatial variation at the state level, which is a useful level for future national or continental studies of a similar kind. The ratio map was calculated by dividing the RS-based AGB value in each pixel by the mean AGB value of all pixels in each of the corresponding states (AGB_{pixel} / $AGB_{statemean}$). Such a ratio map can quantify the spatial variation of AGB across the states compared to the corresponding means. The use of county means refined the accuracy within each state and made the results comparable to previous biomass estimates that used FIA county data as well [56-57] The county means obtained from sampling sizes less than 5 plots were not used; instead, regional AGB mean estimated from remote sensing before the adjustment were used because these few counties were scattered throughout the region.

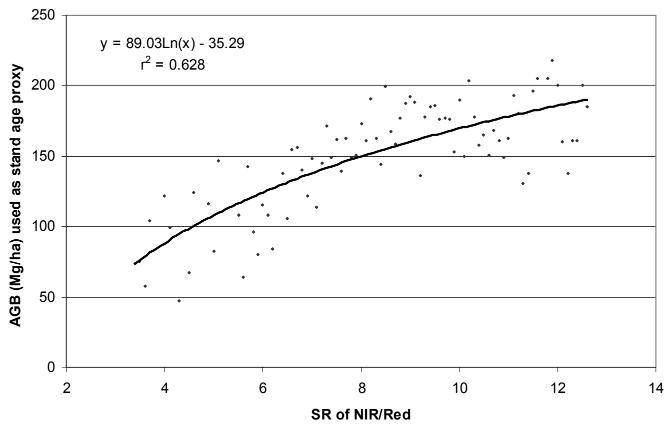

Fig. 3. Relationship between simple ratio (SR) of near infrared reflectance to red reflectance and the Forest Inventory and Analysis (FIA) plot aboveground biomass (AGB, dry weight) within the sampling area. This relationship was used to produce an intermediate product, initial AGB, for age map creation after constrained by regional age structure obtained from FIA data (see Fig. 4).

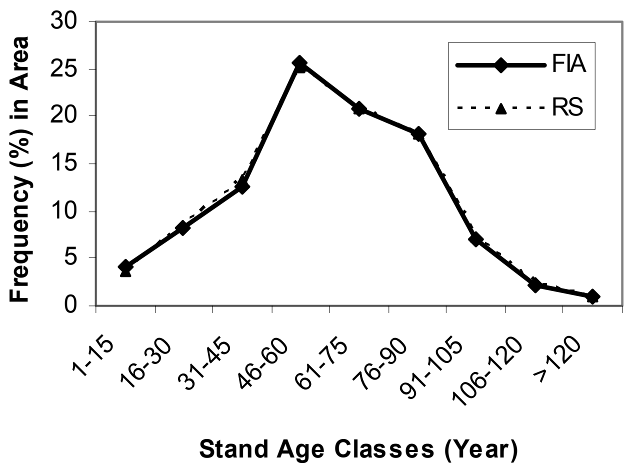

Fig. 4. Comparison of frequency distributions (in area) between reconstructed regional stand-age classes from remote sensing (RS) based initial aboveground biomass (AGB, dry weight) estimates and from 5,502 USDA Forest Service, Forest Inventory and Analysis (FIA) field plots.

a)

3	3	2
2	1	2
1	1	3

b)

1.5	1.5	1
1	0.5	1
0.5	0.5	1.5

c)

6	6	4
4	2	4
2	2	6

Fig. 5. Remote sensing derived aboveground biomass (AGB) density (Mg ha^{-1}) was spatially adjusted by multiplying the FIA derived mean AGB density through a ratio map across the region. In this example for a 3x3 window: i) the mean AGB density estimated from remote sensing (a) can be calculated (e.g., = 2); ii) the ratio map (b) can be developed (AGB_{pixel} / AGB_{mean}); and iii) assuming the mean AGB density calculated from FIA plots within the 3x3 window was 4, the adjusted AGB map (c) was obtained (e.g., ratio map * 4) (From Zheng et al. 2007).

2.8 Model validation and evaluation

Model validation was performed within the ETM+ area using the independent plot AGB values in the reserved dataset. Evaluation of model outputs at state and regional levels were conducted by comparing our final AGB estimates before and after adjustment using FIA county means to the corresponding values obtained from FIA data. The county's AGB means were calculated from the 6,703 FIA plots across the 6 states.

3 RESULTS AND DISCUSSIONS

3.1 Model results

The plot-level empirical model developed from the ETM+ sensor (fine-resolution) was applied to the entire region using MODIS data (after calibrated with the ETM+, Fig. 1, step 2) (which is a coarser resolution) because good correlations existed for remotely sensed information between the two sensors (Table 1). While the reflectance in the infrared band between the sensors has the highest correlation ($r = 0.742$), NDVIc ($r = 0.524$) has a much lower correlation than that for NDVI ($r = 0.682$) because the calculation of NDVIc involves an additional middle infrared band. Our results agree well with a previous study in Central China that a high correlation ($r = 0.788$) was found in NDVI between MODIS and ETM+ [24] It was appropriate to quantify the correlation between the NDVIc values calculated from the MODIS and ETM+ (after aggregating the ETM+ product to the same resolution of MODIS) without calibrating individual bands that are involved. Values of NDVIc calculated using after-calibrated reflectance can be incorrect and misleading because it destroys the inherent relationships among the bands' reflectance.

Our results suggest that stand age, NDVIc, and blue reflectance are the best combination for estimating AGB (Eq. 1, N = 250, $P < 0.001$) in the region.

$$AGB = 392.11 * NDVIc + 1.27 * AGE + 1173.35 * BLUE - 260.95 \qquad r = 0.619, \quad [1]$$

Age factor alone explained 28.3% of the variance. The addition of NDVIc and reflectance in blue band increased the value to 36.9% and 38.3%, respectively. Previous studies also indicated that mIR band centered at 1600 nm was a good predictor of tree biomass [46]

Model validation using data in the reserved group indicated a moderate correlation between the ground-based AGB and the satellite-based AGB but the correlation was still statistically significant ($P < 0.001$) due to a relatively large sample size (Fig. 6). The model tended to overestimate AGB at the low end and underestimate AGB at the high end (> 210 Mg/ha). Although the estimation errors remained large at plot level, we expect much smaller errors in our final adjusted AGB estimates across the region at 1-km resolution. The accuracy and precision of an AGB estimate for a particular point is sometimes of less interest than geographic patterns, spatial distributions, and trends of AGB over entire region for large scale applications.

An approximately linear relationship between age and biomass can be assumed because the regional age structure is relatively young (mean age = 61 years old, Fig. 4) and the biomass in most of the forests has probably not reached an expected asymptotic [50] Recent FIA data suggested that trees greater than 100 years old of age accounted for 4.2% across the region. Across the region, stand age derived from MODIS SR and further constrained by the FIA-derived regional age structure (Fig. 4) was moderately correlated with MODIS blue band and NDVIc (r^2 = 0.270 and 0.377, respectively).

Further division between coniferous and deciduous plots did not improve the predictive power although previous studies in the Great Lakes region suggested that separate models for coniferous and deciduous forests might be needed for calculating vegetation indices and AGB when one or more infrared bands were involved [10, 40] Only 3% of the regional forests were classified as coniferous based on 1-km MODIS land-cover map. Plot data indicated that species composition at broad forest types (e.g., conifers vs. deciduous) could slightly improve our empirical model for regional AGB estimates. We hypothesized that species composition could be estimated by comparing the NDVI values obtained in summer season (full canopy) to the values obtained during the time that deciduous trees have no leaves. However, in this region, snow has usually fallen in some part of the region by the time all deciduous trees in the region have lost their leaves. Thus, parameterization of species composition across the entire region using RS is problematic because the spectral characteristics of snow reflectance (high in red band and low in near infrared band) [58] make interpretation of such comparisons difficult.

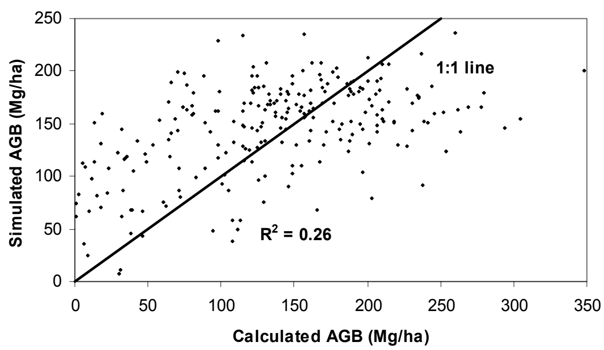

Fig. 6. Comparison between the calculated Forest Inventory and Analysis based aboveground biomass (AGB, dry weight) and the simulated AGB values (N = 249, P < 0.001) using equation 1 before adjustment.

Because the intercept in Eq. 1 was negative, some pixels across the landscape featured AGB values < 0. The majority of these pixels (77%) occurred at the locations adjacent to areas of water or non-forest lands, which tended to have very low AGB values. The pixels with negative AGB values were assigned the value 1 Mg/ha AGB. This assignment should have limited effects on regional AGB analysis because such pixels only accounted for small numbers both in terms of AGB value and area occurrence (1.2%).

3.2 Regional AGB estimates

We estimated that the mean AGB density in the New England states was 120 Mg/ha (Std. = 54) with a total AGB storage of 1,837 teragrams (10^{12}, dry weight) in 2001. Within a 95% percentile, estimated AGB ranged from 15 to 240 Mg/ha, which compares well with the FIA plot data that ranged from 9 to 267 Mg/ha (Figs. 7a & 7b). These curves result from an 11-point running average. Both AGB distribution curves were in a unimodal shape similar to the frequency distribution of forest age structure developed from 2001 FIA data in the region as expected (Fig. 4). About 12.4% of forests were 30 years old, 38.4% and 38.8% were between 30 and 60 years, and between 60 and 90 years of age, respectively. Few forests were greater than 100 years old (4.2% in area, Fig. 4).

RS-based AGB estimates before adjustment generated a regional mean density value of 127 Mg/ha, about 3.2% higher than that (123 Mg/ha) of FIA-based value with a smaller Std. on average (Table 2). Spatially, the model overestimated the AGB values by 29% in ME while underestimating AGB in the other 5 states (Table 2) by an average of -14.4%. There were two possible causes for this spatial discrepancy. First, it was likely caused by model limitation that underestimated AGB at high end: for example, the maximum reduction in mean AGB value occurs in MA because western MA is dominated by maple-birch-beech ecosystems [27] where high AGB is expected. Second, it could be caused by the difference in reflectance responses among different ecosystem communities: for example, spruce-fir forests are dominant in most parts of ME and a previous study has reported that spruce forests tend to have low reflectance in the 1,600 nm mIR wavelength [58] Our data suggested that mean reflectance in the mIR band for ME was 13% lower than that for the other 5 states. Lower mIR will result in higher than expected NDVIc values (see formula above), and these will lead to overestimating AGB values according to Eq. 1.

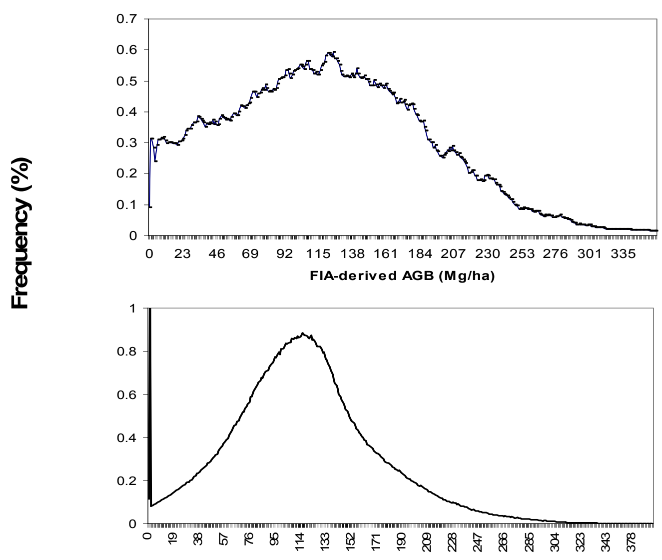

Fig. 7. Frequency distributions of a) Forest Inventory and Analysis (FIA) derived aboveground biomass (AGB) densities, and b) remote sensing (RS) based AGB estimates after adjustment using FIA county AGB means.

Table 2. Statistics of aboveground forest biomass (dry weight, Mg/ha) between the Forest Inventory and Analysis (FIA) plot-based and remote sensing (RS) based estimates of 2001 before and after adjustment using FIA county means for the six New England States, USA.

	Mean (Standard deviation), difference in %[1]		
State	FIA	RS	RS[2]
CT	135 (79)	115 (49), -14.8	130 (57), -3.7
MA	146 (78)	114 (52), -21.9	146 (79), 0.0
ME	103 (59)	133 (46), +28.9	103 (38), 0.0
NH	141 (74)	125 (47), -11.7	138 (54), -2.1
RI	118 (68)	106 (50), -10.2	113 (54), -4.2
VT	142 (69)	123 (46), -13.4	139 (59), -2.1
Overall	123 (69)	127 (48), +3.3	120 (54), -2.4

[1] Compared to FIA estimates.
[2] RS based estimates after adjustment using FIA county means.

This study demonstrated that RS-based AGB estimates can be considerably improved using county means of AGB obtained from the FIA data (Table 2). While the estimated mean AGB density for the region is 2.4% lower than the FIA-derived regional mean density, the AGB means at the state level range from 0% in MA and ME to -4.2% in RI with an average of -2.0%, compared to the FIA-derived state mean densities in the 6 states. Spatial pattern of AGB density is similar to that of stand age across the region, increasing from coast region to inland (Figs. 8a & 8b), except in northern ME where older stands did not have higher AGB. Field data and experimental studies have suggested that AGB accumulation after reaching the peak year can plateau or even decline [50-51, 59-60] The highest variation in AGB estimates occurred in MA and the smallest variation existed in ME, which agreed with the FIA observations (Table 2). Both AGB and stand age maps could provide useful information for fuel-loading estimates across the region, especially the latter because strong relationships between stand age and fuel loading have been reported [16, 61-63]

a) b)

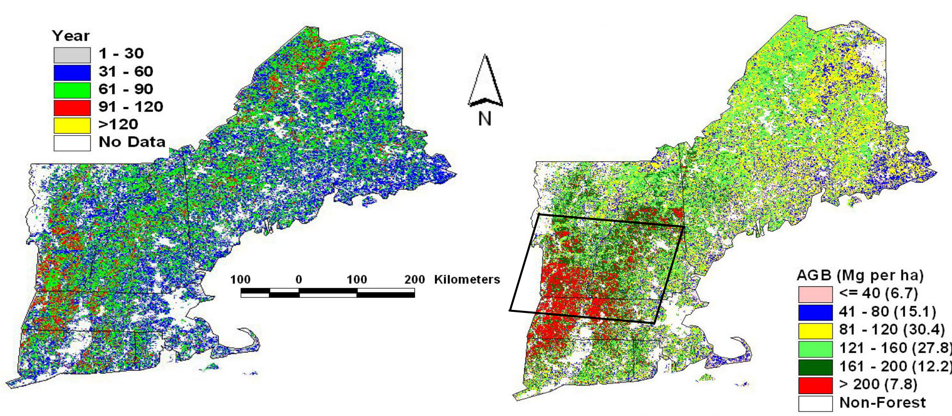

Fig. 8. Spatial distributions of stand age (a) and aboveground biomass (AGB, Mg/ha) estimates (b) in 6 New England states, USA. Numbers in the parentheses are frequency distributions in terms of percentage. The rectangular box shows the area of the full ETM+ scene within which the models were developed. The other solid lines indicate state boundaries.

a)

b)

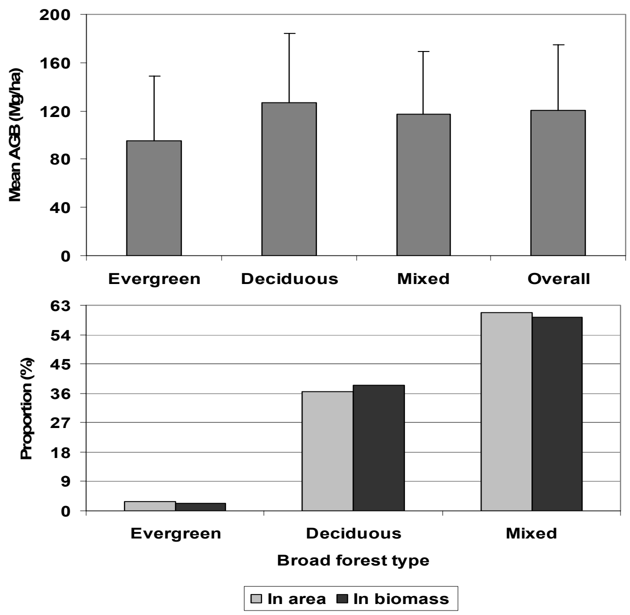

Fig. 9. Comparisons of mean aboveground biomass (AGB, dry weight) density (Bars represent one standard deviation) among broad forest types (a) and proportion of occupancy and AGB storage comparing to total forestland and total regional AGB (b).

We could not assess the accuracy of our MODIS based maps of stand age and AGB because of lack of ground observations at 1-km resolution. However, our methodology provided estimates across the region that are well constrained by the age frequency distributions and almost identical to municipality-level mean AGB values, compared to those obtained from FIA, and with small errors at the state level, which is desirable information for large scale carbon related studies and fuel-loading assessments. Stand age and AGB maps driven by remote sensing and constrained by inventory data could be valuable for pursuing spatial and temporal analyses at regional and national levels because of the increasing availability of satellite data and periodical updates in the FIA database.

Our predicted regional AGB map indicated that high AGB densities were observed along the Appalachian Mountains starting from northwestern CT to the Green Mountains in VT and White Mountains in NH. Low AGB densities were concentrated in the Downeast area of ME and Cape Cod of MA (Fig. 8b). The majority of New England forests (58.2%) were in the range of 80 to 160 Mg/ha, with only about 7% of the forests featuring AGB ≤ 40 Mg/ha and 8% of forests with AGB > 200 Mg/ha (Fig. 8b).

For the broad forest types that are aggregated from the 2001 MODIS land-cover map, deciduous forests have a mean AGB of 127 Mg/ha (Fig. 9a), 32% higher than that of conifers (96 Mg/ha) with the similar pattern in Std. (57 Mg/ha for deciduous vs. 53 Mg/ha for conifers). Mixed forests have a mean AGB of 117 Mg/ha with a Std. of 52 Mg/ha. With the smallest area occupancy in the region (2.8%), evergreen forests contained about 2.2% of the total AGB while mixed forests contained 59.2% AGB with about 61% area occupancy. Deciduous forests featured 39% of AGB but occupied about 36% of the area (Fig. 9b).

4 CONCLUSIONS

The combination of remote sensing imagery and national long-term forest inventory data is a practical and effective way to map the ecosystem properties and attributes that are necessary for predicting fuel loading and conducting carbon-related studies in forest ecosystems.

However, the derived empirical relationships can differ from region to region, and time to time, due to variations in sampling pools and differences in ecosystem structure and properties when samples are collected. It is necessary to pursue internal calibrations of reflectance or vegetation indices remotely sensed for the same target at the same time but from two sensors that differ in both spatial and spectral resolutions before the model(s) developed based on fine-resolution satellite data can be applied to a larger area using coarser-resolution data. These calibrations can reduce the uncertainty caused by sensor difference. However, while the calibration between the reflectance for an individual band could be examined after the fine-resolution data were aggregated to the same resolution as the coarser data; calibrations between various vegetation indices calculated from multiple bands (such as, NDVI and NDVIc) should be conducted after the indices were calculated separately without pursuing calibration in each of the involving bands (such pre-calibration can destroy inherent relationships among different bands).

Using FIA-based regional age structure and county means as reference estimates can substantially reduce uncertainty in mapping regional stand age and forest AGB using remote sensing. While remotely sensed information can preserve spatial integrity and variation across landscapes, extensive forest inventory data can furnish unbiased age frequency distributions and AGB means across the landscapes. Using a ratio map to link remote sensing derived estimates with national inventory data is a methodology worth considering for carbon-related studies at large scales.

Acknowledgments

This study was in part funded by the USDA Forest Service, RWU4104, through grant 05-DG-11242343-074. We thank the USDA Forest Service, Forest Inventory and Analysis Program for use of plot locations (reference MOU 05-SU-FIA02), Elizabeth LaPoint for GIS assistance, and we also thank Michael Nichols and James Smith for additional information about the FIA data.

References

[1] IPCC, "Climate Change 2001: The Scientific Basis," in *Contribution of Working Group I to the Third Assessment Report of the Intergovernmental Panel on Climate Change*, Houghton, J.T., Y. Ding, D.J. Griggs, M. Noguer, P.J. van der Linden, X. Dai, K. Maskell, and C.A. Johnson, Eds., Cambridge University Press, New York, 881pp. Last accessed March 20, 2007, http://www.grida.no/climate/ipcc_tar/wg1/099.htm.

[2] S. C. Wofsy and R. C. Harriss, "The North American Carbon Program (NACP): Report of the NACP Committee of the U.S. Interagency Carbon Cycle Science Program," Washington, DC. U.S. Global Change Research Program. 56 p. Last accessed Mar. 17, 2007, http://www.nacarbon.org/nacp/documents.html.

[3] US Environmental Protection Agency, "Inventory of U.S. Greenhouse Gas Emissions and Sinks: 1990-2004," EPA 430-R-06-002. Office of Atmospheric Programs, Washington, DC. Last accessed Mar. 17 2007, http://epa.gov/climatechange/emissions/usinventoryreport.html.

[4] R. A. Birdsey, "Carbon accounting rules and guidelines for the United States forest sector," *J. Environ. Qual.* **35**(4), 1518-1524 (2006) [doi:10.2134/jeq2005.0193]

[5] Maine Department of Environmental Protection, "A Climate Action Plan for Maine 2004: A report to the joint standing committee on Natural Resources of the Maine Legislature Pursuant to PL 2003 Chapter 237," Volumes 1-2. Last accessed Mar. 17, 2007, http://maineghg.raabassociates.org/finalplan.asp.

[6] S. W. Running, R. Nemani, D. L. Peterson, L. E. Bend, D. F. Potters, L. L. Pierce, and M. A. Spanner, "Mapping regional forest evapotranspiration and photosynthesis by coupling satellite data with ecosystem simulation," *Ecology* **70**(4), 1090-1101 (1989) [doi:10.2307/1941378]
[7] S. D. Prince, and S. N. Goward, "Global primary production: a remote sensing approach," *J. Biogeogr.* **22**(4-5), 815-835 (1995) [doi:10.2307/2845983]
[8] W. B. Cohen, T.A. Spies, R. J. Alig, D. R. Oetter, T. K. Maiersperger, and M. Fiorella, "Characterizing 23 years (1972-1995) of stand replacement disturbance in western Oregon forests with Landsat imagery," *Ecosystems* **5**(2), 122-137 (2002) [doi:10.1007/s10021-001-0060-X]
[9] X. Xiao, D. Y. Hollinger, J. Aber, M. Goltz, E.A. Davidson, Q. Zhang, and B. Moore III, "Satellite-based modeling of gross primary production in an evergreen needleleaf forest," *Rem. Sens. Environ.* **89**(4), 519-534 (2004) [doi:10.1016/j.rse.2003.11.008]
[10] D. Zheng, J. Rademacher, J. Chen, T. Crow, M. Bresee, J. LeMoine, and S-R Ryu, "Estimating aboveground biomass using Landsat 7 ETM+ data across a managed landscape in northern Wisconsin, USA," *Rem. Sens. Environ.* **93**(3), 402-411 (2004) [doi:10.1016/j.rse.2004.08.008]
[11] L. S. Heath, J. E. Smith, and R. A. Birdsey, "Carbon trends in U.S. forest lands: A context for the role of soils in forest carbon sequestration," in *The Potential of US Forest Soils to Sequester Carbon and Mitigate the Greenhouse Effect* J. M. Kimble, others, Eds. CRC Press LLC, Boca Raton, FL, pp. 35-45, (2003).
[12] S. K. Thompson, *Sampling*, John Wiley & Sons, New York (2002).
[13] W. A. Bechtold, and P. L. Patterson, "The enhanced forest inventory and analysis program--national sampling design and estimation procedures," *Tech. Report No. SRS-80*, USDA Forest Service Southern Research Station, (2005).
[14] D. Zheng, S. D. Prince, and T. Hame, "Estimating net primary production of boreal forests in Finland and Sweden from field data and remote sensing," *J. Veg. Sci.* **15**(2), 161-170 (2004) [doi:10.1658/1100-9233(2004)015[0161:ENPPOB]2.0.CO;2]
[15] R. V. Soares, A. C. Batista, and L. J. Souza, "Fuel modeling in *Eucalyptus dunnii* plantations in Tres Barras county, SC, Brazil," *Ceme* **9**(2), 231-245 (2003).
[16] S.-R. Ryu, J. Chen, D. Zheng, M. K. Bresee, and T. R. Crow, "Simulating the effects of prescribed burning on fuel loading and timber production in managed northern Wisconsin forests," *Ecol. Model.* **196**(3-4), 395-406 (2006) [doi:10.1016/j.ecolmodel.2006.02.013]
[17] USDAFS, "Quick briefing on the Enhanced FIA Program," last accessed March 20, 2007, http://fia.fs.fed.us/library/briefings-summaries-overviews/.
[18] S. A. Sader, R. B. Waide, W. T. Lawrence, and A. T. Joyce, "Tropical forest biomass and successional age class relationships to a vegetation index derived from Landsat TM data," *Rem. Sens. Environ.* **28**, 143-156 (1989) [doi:10.1016/0034-4257(89)90112-0]
[19] M. E. Jakubauskas, "Thematic Mapper characterization of lodgepole pine seral stages in Yellowstone National Park, USA," *Rem. Sens. Environ.* **56**(2), 118-132 (1996) [doi:10.1016/0034-4257(95)00228-6]
[20] M. A. Lefsky, D. Harding, W. B. Cohen, G. Parker, and H. H. Shugart, "Surface lidar remote sensing of basal area and biomass in deciduous forests of eastern Maryland, USA," *Rem. Sens. Environ.* **67**(1), 83-98 (1999) [doi:10.1016/S0034-4257(98)00071-6]
[21] M. K. Steininger, "Satellite estimation of tropical secondary forest above-ground biomass: data from Brazil and Bolivia," *Int. J. Rem. Sens.* **21**(6-7), 1139-1157 (2000) [doi:10.1080/014311600210119]
[22] C. A. D. Sannier, J. C. Taylor, and W. D. Plessis, "Real-time monitoring of vegetation biomass with NOAA-AVHRR in Etosha National Park, Namibia, for a

fire risk assessment," *Int. J. Rem. Sens.* **23**(1), 71-89 (2002) [doi:10.1080/01431160010006863]

[23] G. Hurtt, X. Xiao, M. Keller *et al.*, "IKONOS imagery for the large scale biosphere-atmosphere experiment in Amazonia (LBA)," *Rem. Sens. Environ.* **88**(1-2), 111-127 (2003) [doi:10.1016/j.rse.2003.04.004]

[24] T. Alexandridis, and Y. Chemin, "Landsat ETM+, Terra MODIS and NOAA AVHRR: Issues of scale and inter-dependency regarding land parameters," Proceedings of Asian Conference on Remote Sensing, Kathmandu, Nepal, 25-29 November, (2002).

[25] D. P. Turner, S. Ollinger, M.-L. Smith, O. Krankina, and M. Gregory, "Scaling net primary production to a MODIS footprint in support of Earth observing system product validation," *Int. J. Rem. Sens.* **25**(10), 1961-1979 (2004) [doi:10.1080/0143116031000150013]

[26] R. B. Jackson, J. Canadell, J. R. Ehleringer, H. A. Mooney, O. E. Sala, and E.D. Schulze, "A global analysis of root distributions for terrestrial biomes," *Oecologia* **108**(3), 389-411 (1996) [doi:10.1007/BF00333714]

[27] L. C. Irland, *The Northeast's Changing Forest*, Harvard University Press, Cambridge, Massachusetts, (1999).

[28] M. G. New, M. Hulme, and P. D. Jones, "Representing 20th century space-time climate variability II: development of 1901-96 monthly grids of terrestrial surface climate," *J. Clim.* **13**(13), 2217-2238 (2000) [doi:10.1175/1520-0442(2000)013<2217:RTCSTC>2.0.CO;2]

[29] J. E. Smith, L. S. Heath, K. E. Skog, and R. A. Birdsey, "Methods for calculating forest ecosystem and harvested carbon with standard estimates for forest types of the United States" *Tech. Report No. NE-343*, USDA Forest Service, Northeastern Research Station, (2006).

[30] USFS, "Forest Inventory and Analysis National Core Field Guide: Version 3.0," last accessed May 24, 2007, http://fia.fs.fed.us/library/field-guides-methods-proc/docs/2006/core_ver_3-0_10_2005.pdf.

[31] J. C. Jenkins, D. C. Chojnacky, L. S. Heath, and R. A. Birdsey, "Comprehensive database of diameter-based biomass regressions for north American tree species" *Tech. Report No. NE-319* (USDA Forest Service, Northeastern Research Station, 2004).

[32] NASA, "Landsat 7 Science data users handbook. Ch. 11 - data products," last accessed March 20, 2007, http://ltpwww.gsfc.nasa.gov/IAS/handbook/handbook_htmls/chapter11/chapter11.html.

[33] USGS-NASA, "*Distributed Active Archive Center*," Land Processes, last accessed March 20, 2007, http://lpdaac.usgs.gov/main.asp.

[34] J. Dong, R. K. Kaufmann, R. B. Myneni, C. J. Tucker, P. E. Kauppi, J. Liski, W. Buermann, V. Alexeyev, and M. K. Hughes, "Remote sensing estimates of boreal and temperate forest woody biomass: Carbon pools, sources, and sinks," *Rem. Sens. Environ.* **84**(3), 393-410 (2003) [doi:10.1016/S0034-4257(02)00130-X]

[35] P. Bettinger, and R. Hayashi, "Estimation of above-ground biomass with remotely sensed imagery: A brief literature review." *Tech. Report No. 25*, Center for Forest Business, University of Georgia, (2006).

[36] D. S. Lu, "The potential and challenge of remote sensing-based biomass estimation," *Int. J. Rem. Sens.* **27**(7), 1297-1328 (2006) [doi:10.1080/01431160500486732]

[37] R. L. Lawrence, and W. J. Ripple, "Comparisons among vegetation indices and bandwise regression in a highly disturbed, heterogeneous landscape: Mount St. Helens, Washington," *Rem. Sens. Environ.* **64**(1), 91-102 (1998) [doi:10.1016/S0034-4257(97)00171-5]

[38] J. W. Rouse, R. H. Haas, J. A. Schell, and D. W. Deering, "Monitoring vegetation systems in the Great Plains with ERTS," Third ERTS Symposium, Volume 1, pp. 48-62, (1973).

[39] R. Nemani, L. Pierce, S. W. Running, and L. Band, "Forest ecosystem processes at the watershed scale: sensitivity to remotely-sensed leaf area index estimates," *Int. J. Rem. Sens.* **14**(13), 2519-2534 (1993) [doi:10.1080/01431169308904290]

[40] K. S. Fassnacht, S. T. Gower, M. D. MacKenzie, E. V. Nordheim, and T. M. Lillesand, "Estimating the leaf area index of North Central Wisconsin forests using the Landsat Thematic Mapper," *Rem. Sens. Environ.* **61**(2), 229-245 (1997) [doi:10.1016/S0034-4257(97)00005-9]

[41] N. J. Lee, and K. Nakane, "Forest vegetation classification and biomass estimation based on Landsat TM data in mountainous region of west Japan," in *The Use of Remote Sensing in the Modeling of Forest Productivity* H. L. Gholz, K. Nakane, H. Shimoda, Eds. Kluwer, Dordrecht, pp. 159-171, (1997).

[42] S. T. Gower, C. J. Kucharik, and J. M. Norman, "Direct and indirect estimation of leaf area index, f_{apar}, and net primary production of terrestrial ecosystems," *Rem. Sens. Environ.* **70**(1), 29-51 (1999) [doi:10.1016/S0034-4257(99)00056-5]

[43] USGS, "Seamless data distribution," last accessed March 20, 2007, http://seamless.usgs.gov/website/seamless/viewer.php.

[44] P. Muukkonen, and J. Heiskanen, "Biomass estimation over a large area based on standwise forest inventory data and ASTER and MODIS satellite data: A possibility to verify carbon inventories," *Rem. Sens. Environ.* **107**(4), 617-624 (2007) [doi:10.1016/j.rse.2006.10.011]

[45] D. Zheng, L. S. Heath, and M. J. Ducey, "Forest biomass estimated from MODIS and FIA data in the Lake States: MN, WI, and MI, USA," *Forestry* **80**(3), 265-278 (2007) [doi:10.1093/forestry/cpm015]

[46] J. Ardo, "Volume quantification of coniferous forest compartment using spectral radiance recorded by Landsat Thematic Mapper," *Int. J. Rem. Sens.* **13**(9), 1779-1786 (1992) [doi:10.1080/01431169208904227]

[47] P. Muukkonen, and J. Heiskanen, "Estimating biomass for boreal forests using ASTER satellite data combined with standwise forest inventory data," *Rem. Sens. Environ.* **99**(4), 434-447 (2005) [doi:10.1016/j.rse.2005.09.011]

[48] L. A. Schulte, T. R. Crow, J. Vissage, and D. Cleland, "Seventy years of forest change in the northern Great Lake Region, USA," in *Meeting Emerging Ecological, Economic, and Social Challenges in the Great Lakes Region: Popular Summaries.* L. J. Buse, A. H. Perera, Eds. Ontario Forest Research Institute, Sault Ste. Marie, Ontario, Canada, For. Res. Inf. Pap. 155., pp. 99-101, (2003).

[49] J. M. Long, and J. Turner, "Aboveground biomass of understory and overstory in an age sequence of four Douglas-Fir stands," *J. Appl. Ecol.* **12**, 179-188 (1975) [doi:10.2307/2401727]

[50] P. G. Jarvis, and J. W. Leverenz, "Productivity of temperate, deciduous and evergreen forests," in *Physiological Plant Ecology* O. Lange, P. Nobel, C. Osmond, H. Ziegler, Eds. Springer-Verlag, New York, pp. 233-280, (1984).

[51] D. Pare, and Y. Bergeron, "Above-ground biomass accumulation along a 230-year chronosequence in the southern portion of the Canadian boreal forest," *J. Ecol.* **83**(6), 1001-1007 (1995) [doi:10.2307/2261181]

[52] P. E. Dennison, D. A. Roberts, and J. C. Regelbrugge, "Characterizing chaparral fuels using combined hyperspectral and synthetic aperture radar," Proc. 9th JPL Airborne Earth Science Workshop, JPL, Pasadena, CA, Feb. 23-25, pp. 119-124, (2000).

[53] E. P. Odum, "The strategy of ecosystem development," *Sci.* **164**(3877), 262-270 (1969) [doi:10.1126/Science.164.3877.262]

[54] M. G. R. Cannell, *World forest biomass and primary production data*, Academic Press, London, (1982).
[55] R. H. Waring, and S. W. Running, *Forest ecosystems: analysis at multiple scales* Academic Press, San Diego, ed. 2nd, (1998).
[56] P. Schroeder, S. Brown, J. Mo, R. Birdsey, and C. Cieszewski, "Biomass estimation for temperate broadleaf forests of the US using forest inventory data," *Forest Sci.* **43**(3), 424-434 (1997).
[57] S. L. Brown, P. E. Schroeder, and J. S. Kern, "Spatial distribution of biomass in forests of the eastern USA," *Forest Ecol. Manag.* **123**(1), 81-90 (1999) [doi:10.1016/S0378-1127(99)00017-1]
[58] A. G. Klein, D. K. Hall, and G. Riggs, "Improving snow-cover mapping in forests through the use of a canopy reflectance model," *Hydrol. Process.* **12**(10-11), 1723-1744 (1998) [doi:10.1002/(SICI)1099-1085(199808/09)12:10/11<1723::AID-HYP691>3.0.CO;2-2]
[59] F. H. Bormann, and G. E. Likens, *Pattern and Process in a Forested Ecosystem*, Springer-Verlag New York Inc., New York, (1979).
[60] B. T. Bormann, and R. C. Sidle, "Changes in productivity and distribution of nutrients in a chronosequence at Glacier-Bay national park, Alaska," *J. Ecol.* **78**(3), 561-578 (1990) [doi:10.2307/2260884]
[61] B. R. Sturtevant, J. A. Bissonette, J. N. Long, and D. W. Robert, "Coarse woody debris as a function of age, stand structure, and disturbance in boreal Newfoundland," *Ecol. Appl.* **7**(2), 702-712 (1997) [doi:10.1890/1051-0761(1997)007[0702:CWDAAF]2.0.CO;2]
[62] P. A. M. Fernandes, C. A. Loureiro, and H. S. Botelho, "Fire behaviour and severity in a maritime pine stand under differing fuel conditions," *Ann. For. Sci.* **61**(6), 537-544 (2004) [doi:10.1051/forest:2004048]
[63] G. Zhang, J. Chen, and Z. P. Chen, "A study on the dynamic model of surface fuel loading of the mixed forest of Fir and Sassafras," *Acta Agr. Universitatis Jiangxiensis* **26**(2), 178-180 (2004).

Daolan Zheng received his Ph.D. from the University of Montana, and is a research associate at the University of New Hampshire. His current research interests focus on carbon exchange at multiple scales; applications of remote sensing, GIS, and modeling on terrestrial ecosystems; and land-use change detection. He has authored over 30 publications, and is a member of the AGU.

Linda S. Heath is a research forester and team leader with the USDA Forest Service, Northern Research Station in Durham, NH. She received her BS and MS degrees in forestry from the University of Illinois, and a Ph.D. in Quantitative Resources Management from the University of Washington. She has authored over 80 publications. Her research team provides the official U.S. forest greenhouse gas statistics annually for US EPA's Inventory of US Greenhouse Gas Emissions and Sinks.

Mark J. Ducey is an associate professor at the University of New Hampshire. He received his BA, MFS, and Ph.D. from Yale University. He is the author of 48 journal papers and has written six book chapters and over a dozen extension publications. His current research interests include forest carbon dynamics, modeling tree and forest growth, and sampling of natural resources.